A method for determining material's equivalent stress-strain curve with any axisymmetric notched tensile specimens without Bridgman correction

Shengwen Tu[1], Xiaobo Ren[2], Jianying He[1], Zhiliang Zhang[1]

[1]Department of Structural Engineering, Norwegian University of Science and Technology, Trondheim 7491, Norway
[2]SINTEF Materials and Chemistry, Trondheim 7456, Norway

Highlights

- A correction function is proposed to determine material's equivalent stress-strain curve with any axisymmetric notched tensile specimens.
- No Bridgman correction is needed.
- The proposed correction function can be applied to perfectly plastic materials.
- The proposed correction function can be used to measure the equivalent stress-strain curve of each individual material zone in a weldment.

Nomenclature

a	instantaneous minimum cross-section radius
a_0	initial minimum cross-section radius
d_0	outer diameter of the notched tensile specimen
E	Young's modulus
H	material zone length in the notch region
n	material's hardening exponent
P	tensile load
R	instantaneous notch radius
R_0	initial notch radius
a_0/R_0	initial notch radius ratio
ν	Poisson's ratio
ε_0	yield strain
ε	average true strain
$\overline{\varepsilon^p}$	equivalent plastic strain
ε_N	true strain at necking for smooth round bar specimen
$\varepsilon_{P\max}$	true strain at the maximum tensile load
σ_0	yield stress
$\sigma_{0.2}$	0.2% offset yield stress
σ_T	true stress from smooth round bar specimen
$\sigma_{0.5}$	yield stress corresponding to 0.5% total strain
$\overline{\sigma}$	flow stress
$\sigma_{e,notch}$	engineering stress from an axisymmetric notched tensile specimen
σ_{eq}	von Mises equivalent stress
$\sigma_{T,notch}$	average true stress from an axisymmetric notched tensile specimen
ξ	ratio between the average true stress from an axisymmetric notched tensile specimen and the material's equivalent stress at the same strain

A method for determining material's equivalent stress-strain curve with any axisymmetric notched tensile specimens without Bridgman correction

Shengwen Tu[1], Xiaobo Ren[2], Jianying He[1], Zhiliang Zhang[1]
[1]Department of Structural Engineering, Norwegian University of Science and Technology, Trondheim 7491, Norway
[2]SINTEF Materials and Chemistry, Trondheim 7456, Norway

Abstract
Large deformation analyses of problems such as plastic forming, ductile fracture with finite element method need a full range of material's equivalent stress-strain curve or flow stress-strain curve. The equivalent stress-strain curve determined from the smooth round bar specimen should be corrected after diffuse necking, since tri-axial stress state occurs in the neck. The well-known Bridgman correction method is a candidate, however, it is not accurate as the strain increases. Furthermore, it is impossible to measure the equivalent stress-strain curve of each individual material zone in a weldment with cross weld tensile tests. To cope with these challenges, a correction function and an associated test procedure are proposed in this study. With the proposed procedure, the true stress-strain curve from any axisymmetric notched tensile specimen can be converted to the material's equivalent stress-strain curve accurately and no Bridgman correction is needed. The proposed procedure can be applied to both perfectly plastic and strain hardening materials. The equivalent stress-strain curve of each individual material zone in a weldment can also be measured with the proposed procedure.

Keywords: *equivalent stress-strain curve; notched tensile specimen; weldment; Bridgman correction; testing method.*

1. Introduction

Large deformation analyses of problems such as plastic forming [1, 2], ductile fracture [3-7] with finite element method need a full range of material's equivalent stress-strain curve or flow stress-strain curve. For homogeneous materials, the true stress-strain curve can be measured by performing uniaxial tensile test with smooth round bar specimen or rectangular cross-section specimen [8-12]. However, the determination of the true stress-strain curve of each individual material zone in a weldment is difficult, due to the inhomogeneity of the weldment and the unpredictable fracture location on the cross weld tensile specimen. Zhang, Hauge, Thaulow and Ødegård [13] proposed a method to determine the true stress-strain curve of a weldment with axisymmetric notched tensile specimen. The true stress-strain curve from an axisymmetric notched tensile specimen can be converted to the true stress-strain curve of a smooth round bar specimen by a so-called G factor. The notch can be located either in the base metal, weld metal or possibly the heat affect zone (HAZ).

It is worth noting that whether from a smooth round bar specimen [8-10] or by conversion from an axisymmetric notched tensile specimen [13], the true stress-strain curve deviates from the material's equivalent stress-stress curve, since the tri-axial stress state occurs in the localized region after the onset of diffuse necking [8, 14]. In general, the true stress-strain curve should be corrected. Several approaches have been proposed for the correction of the initially smooth round bar tensile specimen [15-17]. The well-known Bridgman correction method [18] is widely referred in the literature. By assuming a uniform distribution of the equivalent strain in the minimum cross section, Bridgman proposed an analytical solution of stress distribution in the minimum cross section of a necked specimen. Application of the Bridgman correction method is expensive since the current notch radius ratio (the minimum cross section radius a over the notch radius R) a/R should be measured simultaneously during the test [14, 19]. Even with the value of notch radius measured, the equivalent stress-strain curve corrected by the Bridgman correction method is not accurate when the strain is large [19]. Bao [20] performed numerical analysis with a smooth round bar specimen and showed that the stress distribution in the minimum cross-section differed significantly to the Bridgman's analytical solution at the strain $\varepsilon = 0.29$. The inaccuracy of the Bridgman correction method attributes to the assumption that the equivalent strain is uniformly distributed in the minimum cross section.

An alternative method with more accurate results and lower test cost has been proposed recently to measure material's flow stress-strain curve [21]. The authors further studied the axisymmetric notched tensile specimen with numerical analyses and a special notch geometry with $a_0/R_0 = 2$ has been identified. a_0 and R_0 are the initial minimum cross-section radius and the initial notch radius, respectively. With this 'magic' notched tensile specimen and a smooth round bar specimen, the equivalent stress-strain curve of the hardening material can be directly derived with a single G factor and no Bridgman correction is needed. Good agreements between the equivalent stress-strain curves input for numerical analyses and the G-corrected equivalent stress-strain curves with the 'magic' notched tensile specimen have been observed. Similar with the Bridgman correction method, the proposed 'magic' notch method is not accurate for the perfectly plastic or weak hardening material [15].

In the present study, a new correction function is proposed to determine the material's equivalent stress-strain curve with any axisymmetric notched tensile specimens rather than the only 'magic' notch. The proposed correction function depends on the deformation level (the average true strain ε), the true strain corresponding to the maximum tensile load $\varepsilon_{P\max}$ and the initial notch geometry a_0/R_0 of the specimen. Different notch configurations can be used. The proposed correction function herein can also be applied to perfectly plastic materials.

The paper consists of the following sections. In section 2, the axisymmetric notched tensile specimen is introduced, along with the definitions of the specimen geometry used in this study. Details of the numerical procedure and materials used are presented in section 3. Results from the numerical analyses, the influence of notch radius ratio, as well as the derivation of the correction function are presented in section 4. Verification and application of the proposed correction function are discussed in section 5. The main conclusions are summarized in section 6.

2. Axisymmetric notched tensile specimen

The axisymmetric notched tensile specimen has a wide range of applications in characterizing material's mechanical properties [22-25], especially for the metallic material fracture locus measurement in the range of stress triaxiality larger than 1/3 [26-28]. In order to conquer the limitations of the conventional cross weld tensile test, Zhang, Hauge, Thaulow and Ødegård [13] proposed a method to determine the true stress-strain curve of each individual material zone of weldments with the axisymmetric notched tensile specimen. The sketch of an axisymmetric notched tensile specimen is shown in Fig. 1. Due to the existence of a notch on the specimen, the deformation localizes mainly in the notched region under uniaxial tension. During the tensile testing, the average true strain ε is defined by the minimum cross-section area reduction:

$$\varepsilon = 2 \cdot \ln(a_0/a) \tag{1}$$

where a is the instantaneous minimum cross-section radius, which can be measured by a linear variable displacement transducer. The true stress $\sigma_{T,notch}$ and the engineering stress $\sigma_{e,notch}$ from an axisymmetric notched tensile specimen are calculated by dividing the load P by the current minimum cross-section area and the initial minimum cross-section area, respectively.

$$\sigma_{T,notch} = P/\pi a^2 \tag{2}$$

$$\sigma_{e,notch} = P/\pi a_0^2 \tag{3}$$

Recent study by the authors [21] showed that the true stress calculated by Eq. (2) with the axisymmetric notched tensile specimen is independent of the specimen outer diameter d_0 when the geometry condition $d_0 \geq 3.5a_0$ is fulfilled. In order to measure the equivalent stress-strain curve of each individual material zone of a weldment, the authors carried out a series of numerical analyses and found that the true stress from an axisymmetric notched tensile specimen is unique and independent of the material zone length when $a_0 \leq H$. When these geometry requirements are fulfilled, the axisymmetric notched tensile specimen can be characterized by the initial notch radius ratio, a_0/R_0 .

The strategy of the present study is illustrated in Fig. 2. The assumed materials' equivalent stress-strain curves are used for numerical analyses first. Then, the true stress-strain curves output from the numerical analyses are studied to derive the proposed correction function. With the proposed correction function, the true stress-strain curve from an axisymmetric notched tensile specimen can be converted to the material's equivalent stress-strain curve.

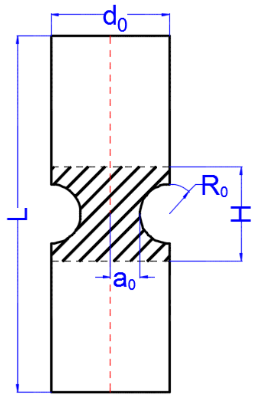

Fig. 1 Geometry of an axisymmetric notched tensile specimen

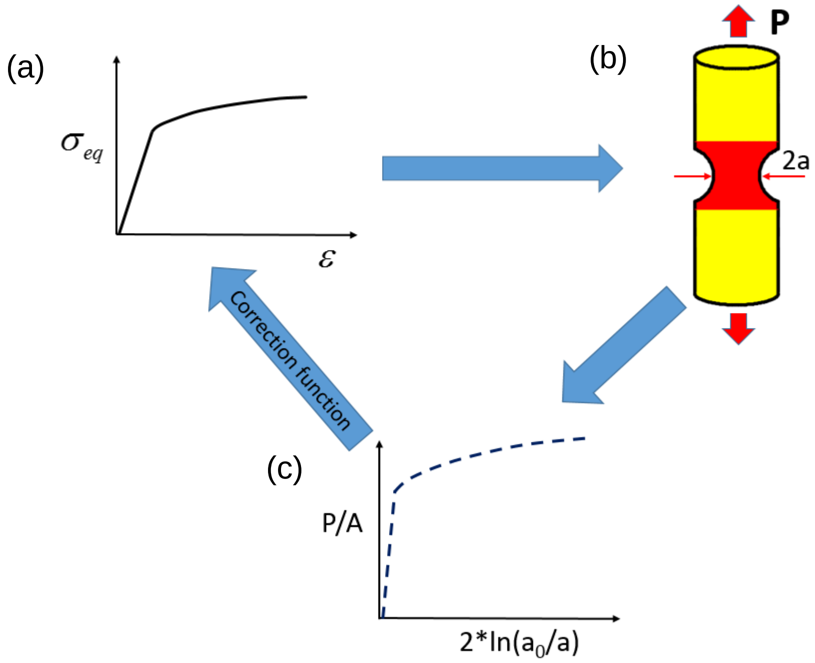

Fig. 2 Layout of the present study: (a) Assumed material's equivalent stress-strain curve; (b) Numerical tensile tests with axisymmetric notched tensile specimens, material in red can be undermatched, overmatched or evenmatched with the base material in yellow; (c) True stress-strain curve for the notched specimen obtained from Fig. 2 (b). With the proposed correction function, true stress-strain curve in Fig. 2 (c) can be corrected back to Fig. 2 (a).

3. Numerical procedure

3.1 Finite element model

A series of numerical analyses of axisymmetric notched tensile specimens with a_0/R_0 varying from 0.25 to 3 have been performed with Abaqus/standard 6.14. $a_0 = 6$ *mm* is used for all the notched tensile specimens, with R_0 varying from 2 to 24 *mm*. The outer diameter is 24 *mm*, which meets the geometry requirement: $d_0 \geq 3.5a_0$. Axisymmetric model has been used with the element type CAX4R. Large deformation is accounted. A typical finite element meshes is shown in Fig. 3 for the axisymmetric notched tensile specimen with $a_0/R_0 = 0.5$. Average mesh size in the notch center is 0.5×0.5 *mm* and relative coarse meshes are used in the remaining part. Symmetric boundary condition is applied in the minimum cross-section. The specimen is loaded under displacement control.

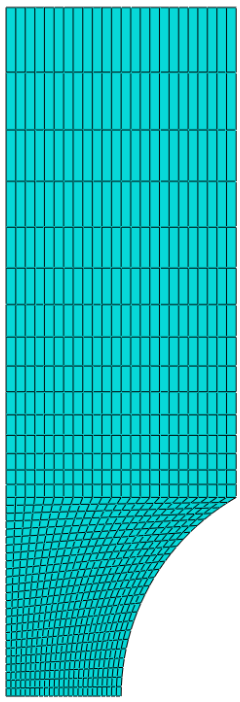

Fig. 3 Mesh of the axisymmetric notched tensile specimen with $a_0/R_0 = 0.5$.

3.2 Materials

The flow stress-strain curves of the materials used in this study are assumed to follow a power law hardening rule [29]:

$$\bar{\sigma} = \sigma_0 \left(1 + \frac{\bar{\varepsilon}^p}{\varepsilon_0}\right)^n \tag{4}$$

where $\bar{\sigma}$, $\bar{\varepsilon}^p$ are the flow stress and the equivalent plastic strain, respectively. $\sigma_0 = E\varepsilon_0$ describes the elastic behavior of the material. The yield stress $\sigma_0 = 400MPa$, the Young's modulus $E = 200\ GPa$, and corresponding yield strain $\varepsilon_0 = 0.002$ have been used together with the Poisson's ratio $\nu = 0.3$, for all the numerical analyses. Hardening of the material is characterized by a single hardening exponent n. In this study, numerical analyses with hardening exponents ranging from 0 to 0.2 have been investigated, representing most engineering materials. For a given hardening exponent n, the flow stress-strain curve can be converted to the equivalent stress-strain curve by Eq. (5):

$$\begin{cases} \sigma_{eq} = \overline{\sigma}, \quad \varepsilon = \overline{\sigma}/E & \overline{\varepsilon^{p}} = 0 \\ \sigma_{eq} = \overline{\sigma}, \quad \varepsilon = \dfrac{\overline{\sigma}}{E} + \overline{\varepsilon^{p}} & \overline{\varepsilon^{p}} > 0 \end{cases} \tag{5}$$

In the following sections, material's equivalent stress-strain curve is calculated by converting the corresponding flow stress-strain curve by Eq. (5). By combining different hardening exponents and initial notch radius ratios (a_0/R_0), in total 30 analyses have been performed to derive the correction function in section 4.

4. Derivation of the correction function

4.1 Normalized $\sigma_{T,notch} - \varepsilon$ and $\sigma_{e,notch} - \varepsilon$ curves from numerical analyses

The true stress-strain curves ($\sigma_{T,notch} - \varepsilon$) calculated by Eq. (2) for the axisymmetric notched tensile specimens are normalized by the yield stress and are presented in Fig. 4 for the perfectly plastic material and Fig. 5 for hardening materials. The corresponding materials' equivalent stress-strain curves are also presented.

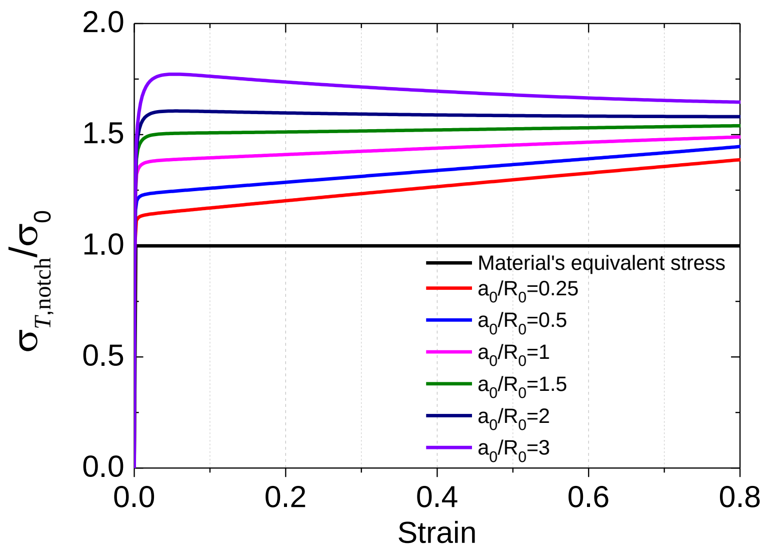

Fig. 4 Normalized $\sigma_{T,notch} - \varepsilon$ curves of the axisymmetric notched tensile specimens for the perfectly plastic material ($n = 0$). The material's equivalent stress-strain curve is denoted as black.

As expected, for axisymmetric notched tensile specimens with the same hardening exponent in Fig. 4 and Fig. 5, the true stress calculated by Eq. (2) is larger than the material's equivalent stress at the same strain, and the sharper notch (larger value of a_0/R_0) yields a larger true stress. It is interesting to note that for the perfectly plastic material shown in Fig. 4, the true stress increases with the increase of the strain for the specimen with $a_0/R_0 < 1.5$. For the specimen with $a_0/R_0 = 3$, the true stress increases when the strain is small, and then decreases as the strain increases. For the specimens with $a_0/R_0 = 1.5$ and $a_0/R_0 = 2$, the true stress increases firstly, and then varies slightly as the strain increases. It indicates that, with a single correction parameter, the true stress output from an axisymmetric notched tensile specimen with $a_0/R_0 = 1.5$ or $a_0/R_0 = 2$ can be converted to the material's equivalent stress. This has been investigated by the authors for hardening materials [21], and the axisymmetric notched tensile specimen with $a_0/R_0 = 2$ has been proved to present a good agreement between the material's equivalent stress-strain curve and the corrected stress-strain curve with a single G factor.

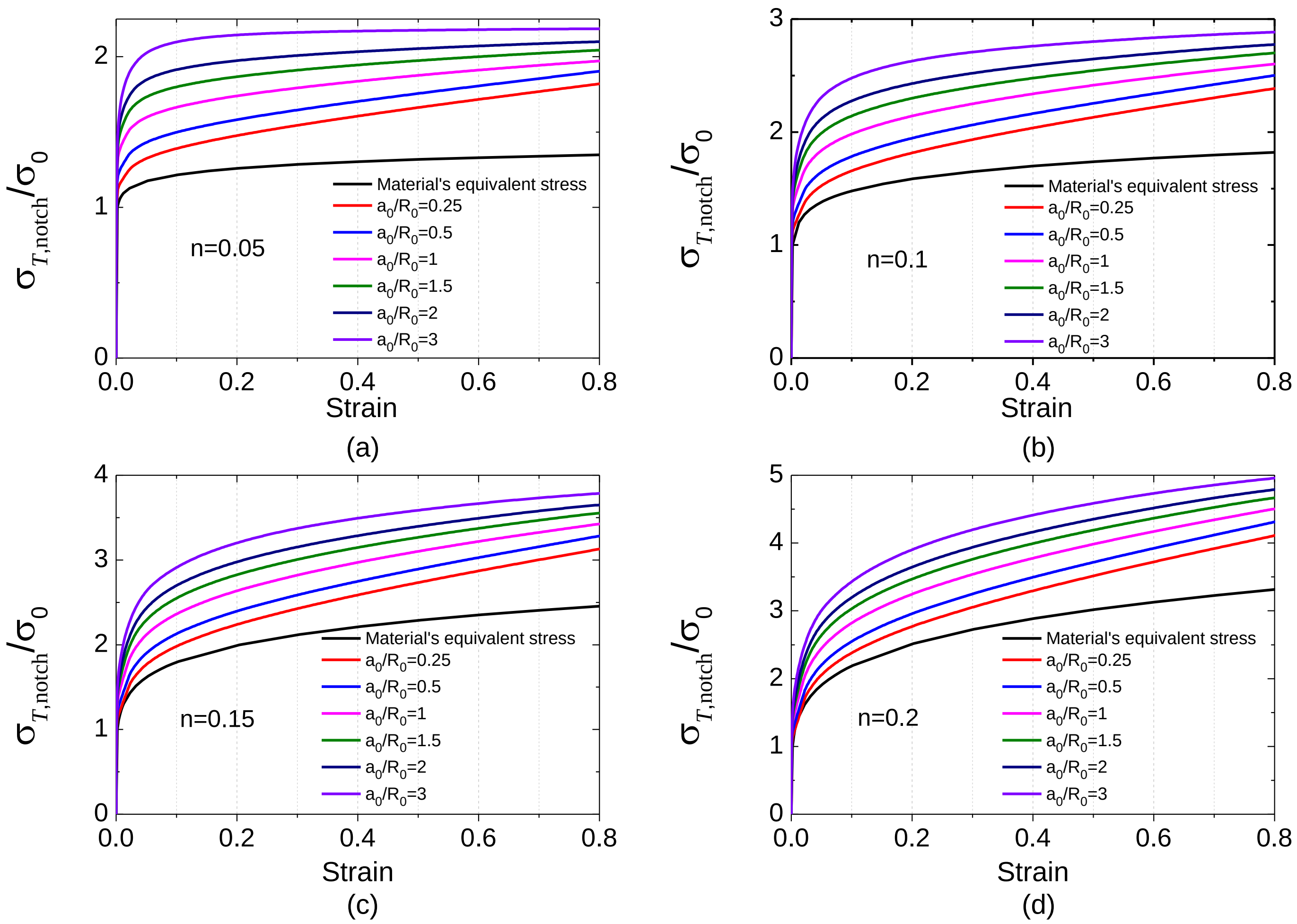

Fig. 5 Normalized $\sigma_{T,notch} - \varepsilon$ curves of axisymmetric notched tensile specimens with different notch configurations: (a) $n = 0.05$; (b) $n = 0.1$; (c) $n = 0.15$; (d) $n = 0.2$. The corresponding materials' equivalent stress-strain curves are shown in black.

Indeed, the effect of the initial notch radius ratio (a_0/R_0) on the resulting true stress-strain curve also occurs for hardening materials shown in Fig. 5. However, it is difficult to observe this phenomenon duo to the materials' strain hardening. The reason for the initial notch radius ratio effect is mainly due to the stress distribution on the minimum cross-section and will not be discussed in this paper.

The normalized engineering stress-true strain curves (normalized $\sigma_{e,notch} - \varepsilon$) of the axisymmetric notched tensile specimens with hardening exponents $n = 0.1$ and $n = 0.2$ are presented in Fig. 6. As expected, the engineering stress decreases after reaching the maximum value, for all the notched tensile specimens. It has been demonstrated that the strain corresponding to the maximum value of the engineering stress is approximately equal to the material's hardening exponent ($\varepsilon_{P\max} \approx n$), independent of the initial notch radius ratio [13, 21]. This is further investigated and a function describes the notch effect on diffuse necking is established in this paper.

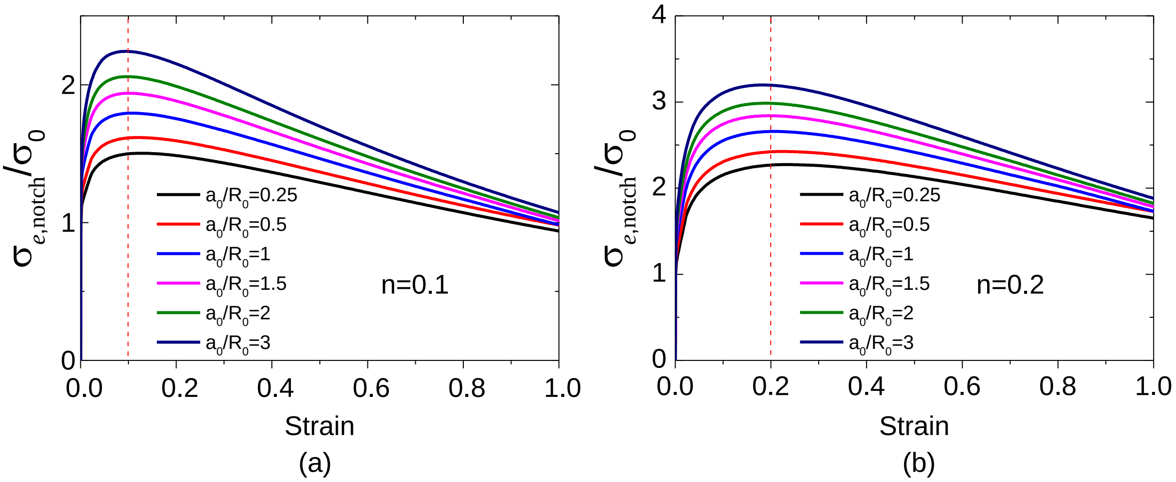

Fig. 6 Normalized $\sigma_{e,notch} - \varepsilon$ curves of axisymmetric notched tensile specimens: (a) $n = 0.1$; (b) $n = 0.2$. The strains corresponding to the maximum engineering stresses are shown with red lines.

4.2 The derivation of the correction function

4.2.1 Normalizing the ratio between the true stress and the material's equivalent stress

The purpose for this study is to provide a simple correction function to convert the true stress-strain curve from an axisymmetric notched tensile specimen to the material's equivalent stress-strain curve. The ratio ξ between the true stress from an axisymmetric notched tensile specimen and the material's equivalent stress in Fig. (4)–(5) are calculated by Eq. (6), with the strain varying from 0.01 to 0.8.

$$\xi = \frac{\sigma_{T,notch}}{\sigma_{eq}}\Big|_{\varepsilon} \tag{6}$$

The ξ versus the strain for the axisymmetric notched tensile specimens with $a_0/R_0 = 3$ and hardening exponents from 0 to 0.2 are presented in Fig. 7. It can be seen in Fig. 7 (a) that the curves for different hardening exponents show similar trend. The values of ξ increases with the increase of the strain initially, and then decreases, for all the materials shown in Fig. 7 (a). By taking the ratio ξ at strain $\varepsilon = 0.8$ as a reference, the curves in Fig. 7 (a) are normalized and the results are presented in Fig. 7 (b). Interestingly, the normalized curves in Fig. 7 (b) collapse into one, except small deviations when the strain is very small. Same behavior of the $\xi - \varepsilon$ curves is also observed in Fig. 8-12 for the notched tensile specimens with a_0/R_0 ranging from 0.25 to 2.

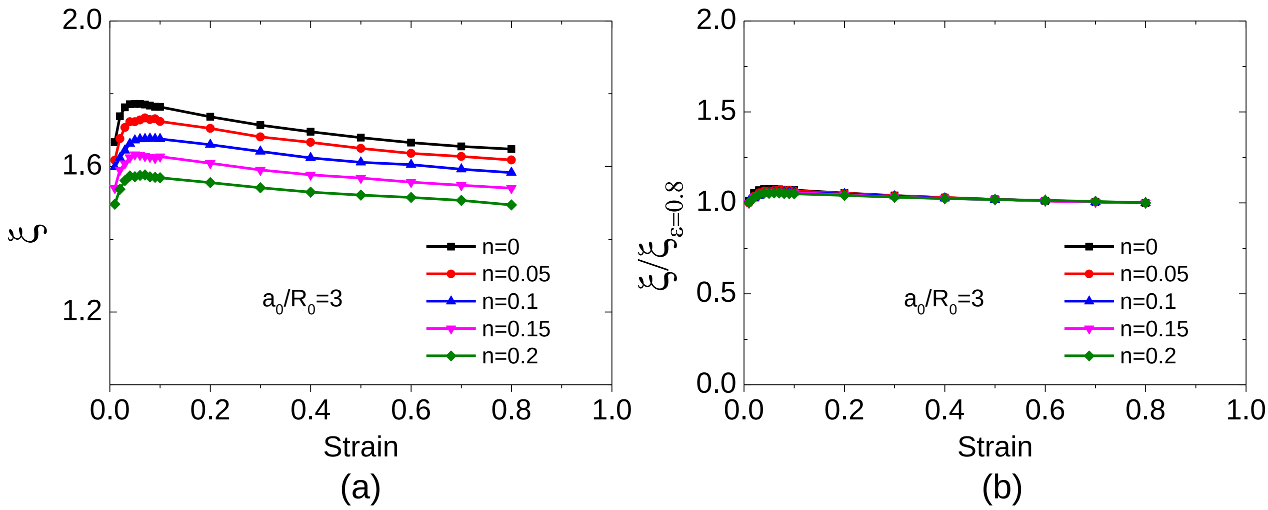

Fig. 7 (a) ξ versus ε for the axisymmetric notched tensile specimen with $a_0/R_0 = 3$ and n ranging from 0 to 0.2; (b) Normalized curves of Fig. 7 (a) by $\xi_{\varepsilon=0.8}$.

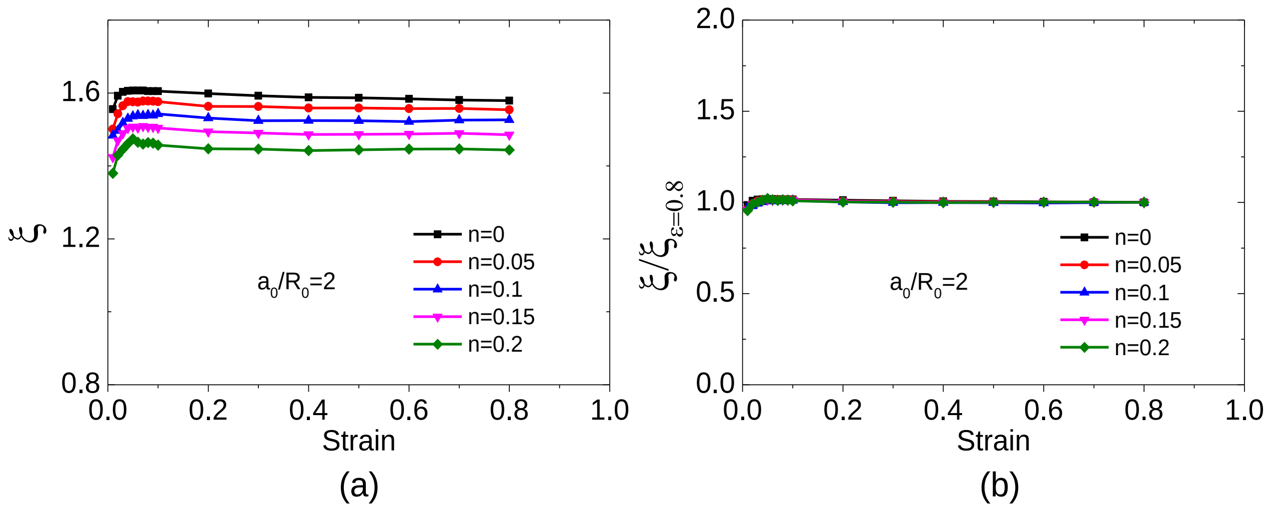

Fig. 8 (a) ξ versus ε for the axisymmetric notched tensile specimen with $a_0/R_0 = 2$ and n ranging from 0 to 0.2; (b) Normalized curves of Fig. 8 (a) by $\xi_{\varepsilon=0.8}$.

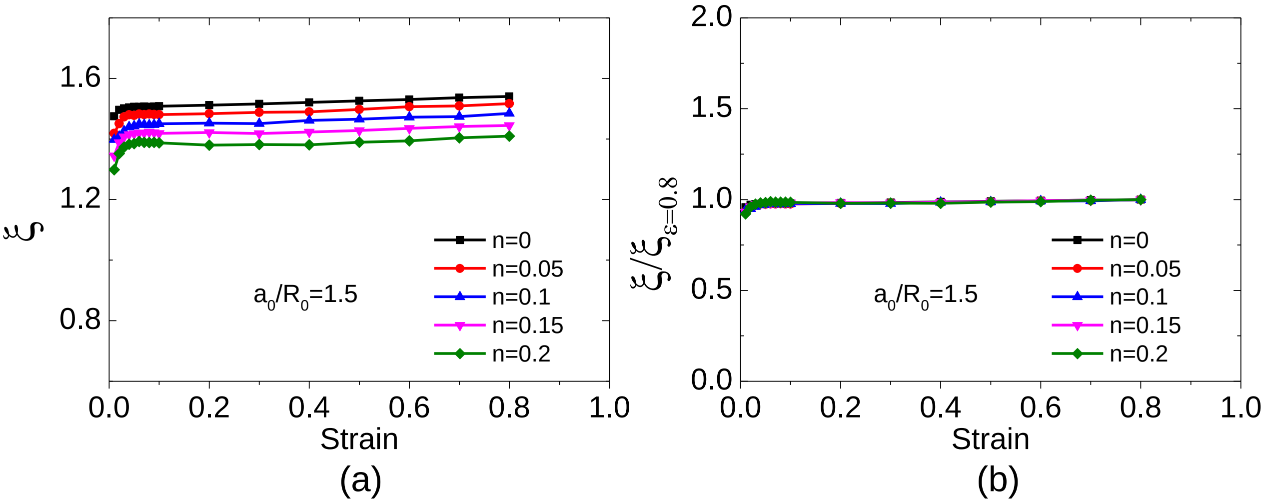

Fig. 9 (a) ξ versus ε for the axisymmetric notched tensile specimen with $a_0/R_0 = 1.5$ and n ranging from 0 to 0.2; (b) Normalized curves of Fig. 9 (a) by $\xi_{\varepsilon=0.8}$.

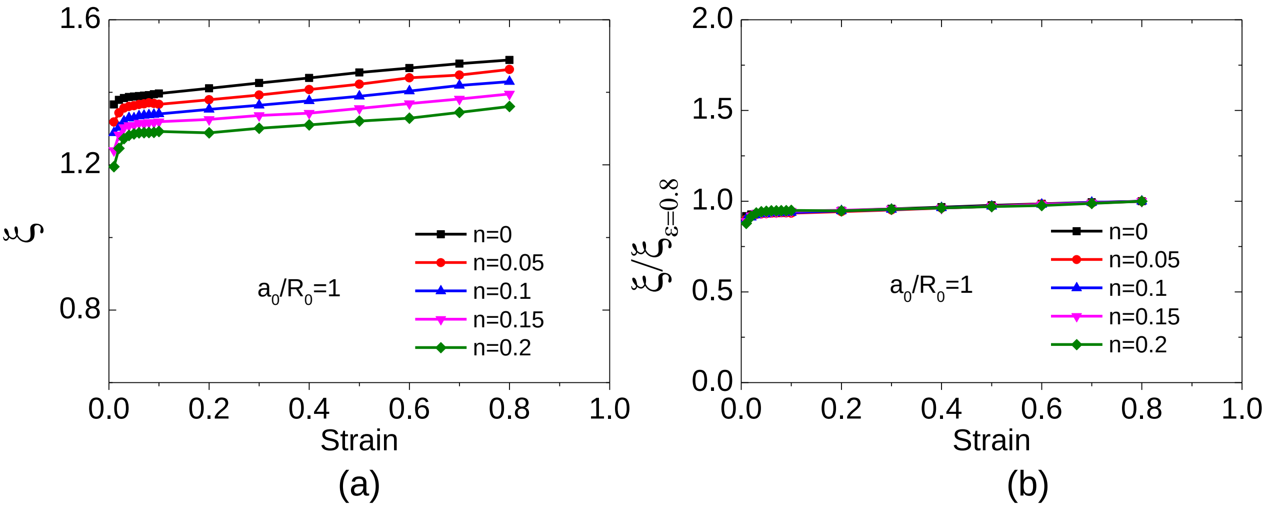

Fig. 10 (a) ξ versus ε for the axisymmetric notched tensile specimen with $a_0/R_0 = 1$ and n ranging from 0 to 0.2; (b) Normalized curves of Fig. 10 (a) by $\xi_{\varepsilon=0.8}$.

The influence of notch radius ratio on the true stress-strain curve of axisymmetric notched tensile specimens has been analyzed previously for the perfectly plastic material. Interestingly, the influence of notch radius ratio (a_0/R_0) can also be observed from the normalized $\xi - \varepsilon$ curves, as seen in Fig. 7 (b)-12 (b). The value of normalized ξ for notched tensile specimens with $a_0/R_0 > 1.5$ decreases as the strain increases, and larger a_0/R_0 corresponds a faster decrease of the normalized ξ . On the contrary, the value of normalized ξ for notched tensile specimens with $a_0/R_0 \le 1.5$ increases with the increase of the strain, and smaller a_0/R_0 yields a faster increase of the normalized ξ. Therefore, we may conclude that the notch radius ratio effect is determined by the notch geometry (a_0/R_0), independent of the material's hardening exponent.

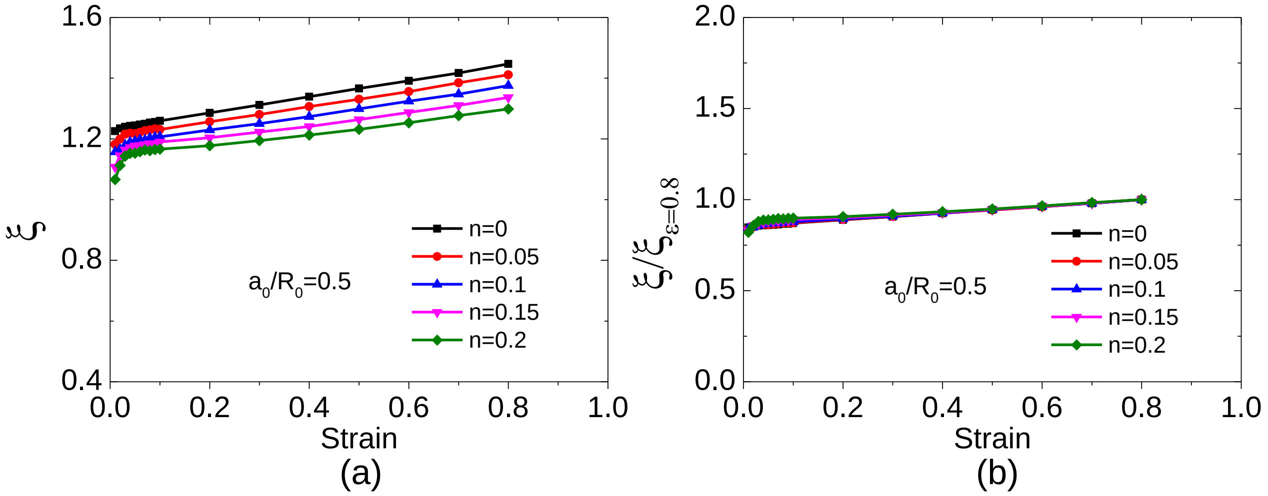

Fig. 11 (a) ξ versus ε for the axisymmetric notched tensile specimen with $a_0/R_0 = 0.5$ and n ranging from 0 to 0.2; (b) Normalized curves of Fig. 11 (a) by $\xi_{\varepsilon=0.8}$.

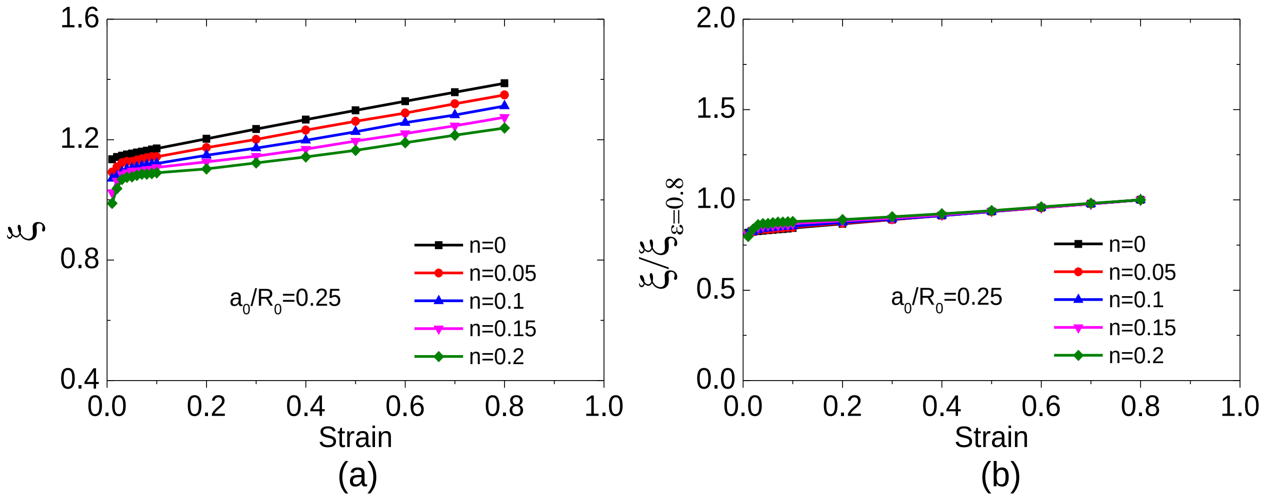

Fig. 12 (a) ξ versus ε for the axisymmetric notched tensile specimen with $a_0/R_0 = 0.25$ and n ranging from 0 to 0.2; (b) Normalized curves of Fig. 12 (a) by $\xi_{\varepsilon=0.8}$.

4.2.2 Normalizing $\xi_{\varepsilon=0.8}$

The ratio between the true stress and the material's equivalent stress at $\varepsilon = 0.8$ (namely the reference points $\xi_{\varepsilon=0.8}$ used in Fig. 7-12) versus the materials' hardening exponents for axisymmetric notched tensile specimens with different notch geometries are shown in Fig. 13, with hardening exponents up to 0.35. For a given axisymmetric notched tensile specimen (a_0/R_0), the value of $\xi_{\varepsilon=0.8}$ decreases with increasing hardening exponent. Very interestingly, for axisymmetric notched tensile specimens with different notch geometries, the curves in Fig. 13 (a) behave similar to each other and can be normalized. By taking the value of $\xi_{\varepsilon=0.8}$ for material with the hardening exponent $n = 0$ ($\xi_{\varepsilon=0.8,n=0}$) as a reference, the curves for axisymmetric notched tensile specimens with different notch geometries in Fig. 13 (a) can be normalized. The corresponding normalized curves are presented in Fig. 13 (b). As it can be seen, the normalized curves in Fig. 13 (b) collapse into one, which can be fitted by Eq. (7):

$$f(n) = -0.22942 \cdot n^2 - 0.36902 \cdot n + 1 \tag{7}$$

where n is the material's hardening exponent. Eq. (7) describes the material's hardening effect on the true stress-strain curves from notched specimen. As mentioned previously, for materials obeying the power law hardening (see Eq. (4)), the hardening exponent n approximately equals to the true strain at the maximum tensile load, $\varepsilon_{P\max}$. We further investigate $\varepsilon_{P\max}$ for each numerical analysis for hardening materials in section 4.1. The $\varepsilon_{P\max}$ for each case is normalized by the hardening exponent n and is plotted against the initial notch radius ratio in Fig. 14. As can be seen, the normalized $\varepsilon_{P\max}$ presents a small scatter at the given a_0/R_0 and decreases with the increase of a_0/R_0, for all the hardening exponents discussed here. Fig. 14 indicates that sharper notch accelerates the diffuse necking, while the shallow notch postpones the diffuse necking. Fig. 14 is then fitted by Eq. (8).

$$\varepsilon_{P\max}/n = 0.0466 \cdot (a_0/R_0)^2 - 0.2515 \cdot (a_0/R_0) + 1.2462 \tag{8}$$

Eq. (8) describes the notch effect on diffuse necking. The strain hardening exponent n can be determined with Eq. (8) when $\varepsilon_{P\max}$ from a notched specimen is measured. For a given notched tensile specimen, the ratio ξ at the strain $\varepsilon = 0.8$ can be calculated, once $\varepsilon_{P\max}$ and the reference value $\xi_{\varepsilon=0.8,n=0}$ is known:

$$\xi_{\varepsilon=0.8} = f(n) \cdot \xi_{\varepsilon=0,8,n=0} \tag{9}$$

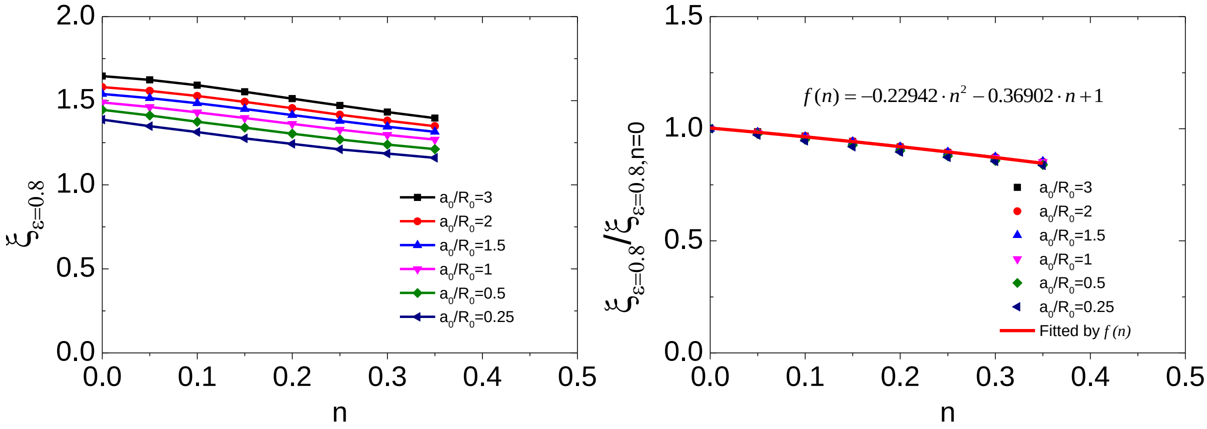

(a) (b)

Fig. 13 (a) $\xi_{\varepsilon=0.8}$ versus n for axisymmetric notched tensile specimens with different notch geometries; (b) Normalized curves of Fig. 13 (a) by $\xi_{\varepsilon=0.8,n=0}$ and are fitted by Eq. (7).

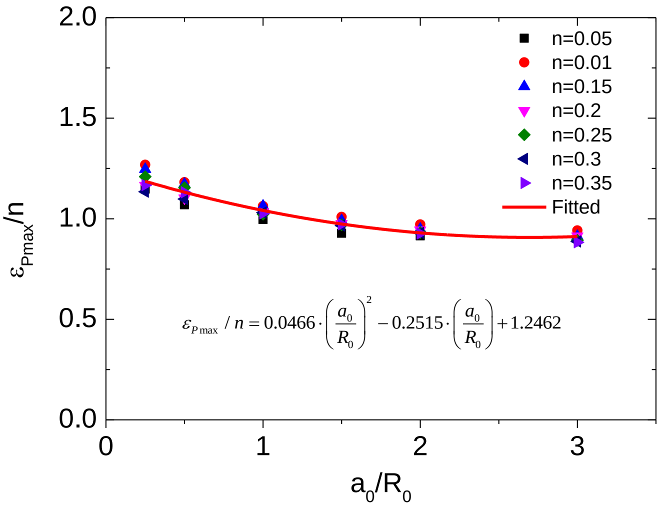

Fig. 14 Strain corresponding to the maximum load is normalized by hardening exponent and is plotted against the initial notch radius ratio.

4.2.3 The proposed correction function

As mentioned previously, for a given axisymmetric notched tensile specimen with different material properties (namely, different hardening exponents), the normalized $\xi-\varepsilon$ curves collapse into one and can be linearly fitted by Eq. (10), as seen in Fig. 7 (b)-12 (b).

$$g_{a_0/R_0}(\varepsilon) = (b_1 * \varepsilon + b_2)_{a_0/R_0} \tag{10}$$

where b_1 and b_2 are the slope and the intersection of Eq. (10), respectively. The subscript in Eq. (10) denotes the initial notch radius ratio for a given axisymmetric notched tensile specimen. Combining Eq. (9) and (10), the ratio ξ can be written as:

$$\xi = f(n) \cdot \xi_{\varepsilon=0.8,n=0} \cdot g_{a_0/R_0}(\varepsilon) \tag{11}$$

Considering that the $\xi-\varepsilon$ curves in Fig. 7 (a)-12 (a) are normalized by $\xi_{\varepsilon=0.8}$, the product of the second and third term in Eq. (11) returns back to the linear fitted curves for the perfectly plastic materials ($n=0$) in Fig. 7 (a)-12 (a). In this case, $\xi_{\varepsilon=0.8,n=0}$ cancels out and Eq. (11) can be written:

$$\begin{aligned} \xi &= f(n) \cdot g_{a_0/R_0,n=0}(\varepsilon) \\ g_{a_0/R_0,n=0}(\varepsilon) &= \left(b_{1,n=0} \cdot \varepsilon + b_{2,n=0}\right)_{a_0/R_0} \end{aligned} \tag{12}$$

where $b_{1,n=0}$ and $b_{2,n=0}$ are the slope and intersection from the linear fitting of the curves for $n=0$ in Fig. 7 (a)-12 (a), respectively. Corresponding values of $b_{1,n=0}$ and $b_{2,n=0}$ of Eq. (12) are listed in Table 1 and are presented in Fig.15 as functions of the initial notch radius ratio. The value of slope of Eq. (12) decreases with the increase of the initial notch radius ratio; inversely, the value of the intersection increases. The slope represents the notch radius ratio effect, while the intersection infers the stress concentration due to the existence of notch. The data in Fig. 15 (a) and (b) are fitted by Eq. (13) and Eq. (14):

$$b_{1,n=0} = 0.03232\left(\frac{a_0}{R_0}\right)^2 - 0.27\left(\frac{a_0}{R_0}\right) + 0.3866 \tag{13}$$

$$b_{2,n=0} = -0.04084\left(\frac{a_0}{R_0}\right)^2 + 0.3557\left(\frac{a_0}{R_0}\right) + 1.0577 \tag{14}$$

Table 1 Parameters from linear fitting of Fig. 7 (b)-12 (b) by Eq. (10)

a_0/R_0	*Slope*	*Intersection*
	$b_{1,n=0}$	$b_{2,n=0}$
3	-0.135	1.7597
2	-0.0194	1.5985
1.5	0.0529	1.4987
1	0.137	1.3799
0.5	0.2743	1.2299
0.25	0.3143	1.1376

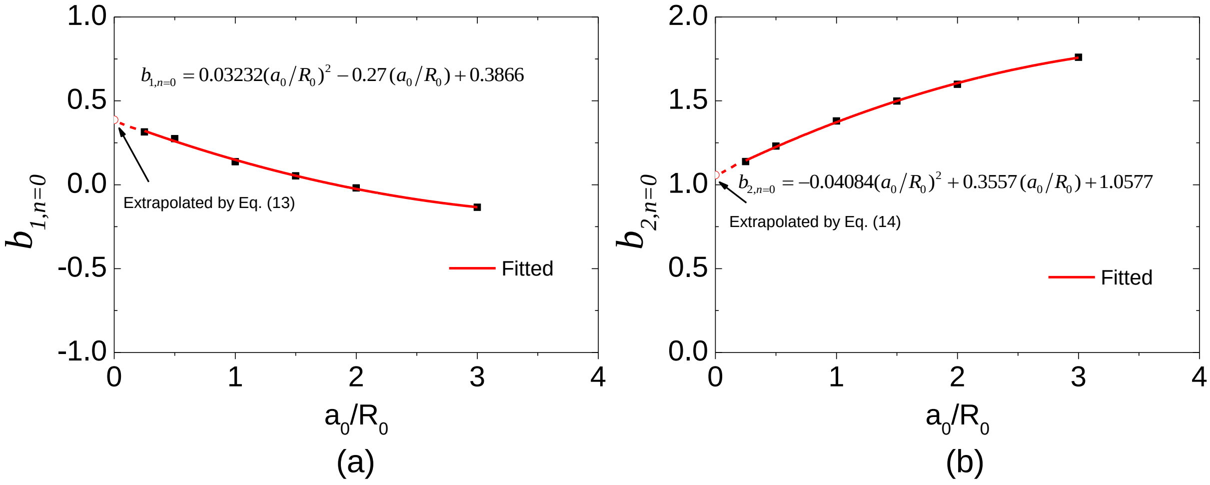

Fig. 15 (a) Slopes of linearly fitted equations of the $\xi-\varepsilon$ curves with n=0 in Fig. 7 (a)-12 (a) versus the initial notch radius ratio a_0/R_0; (b) Intersections of linearly fitted equations of the $\xi-\varepsilon$ curves for n=0 in Fig. 7 (a)-12 (a) versus the initial notch radius ratio a_0/R_0.

Inserting Eq. (13)-(14) into Eq. (12), the ratio ξ between the true stress from an axisymmetric notched tensile specimen and the material's equivalent stress can be written in a general format:

$$\xi=(b_{1,n=0}\cdot\varepsilon+b_{2,n=0})\cdot f(n) \tag{15}$$

Eq. (15) consists of two terms: the first term is related to the initial notch geometry and is a function of the average true strain ε; the second term is a function of the hardening exponent n, considering the material's strain hardening effect. With Eq. (15), the $\sigma_{T,notch}-\varepsilon$ curve from an axisymmetric notched tensile specimen can be converted to the material's equivalent stress-strain curve by Eq. (16). Therefore, Eq. (15) is the proposed correction function.

$$\sigma_{eq}=\frac{\sigma_{T,notch}}{\xi}\Big|_{\varepsilon} \tag{16}$$

It should be noted that the correction function Eq. (16) are derived based on notched specimens and are not accurate for $a_0/R_0=0$, namely the smooth round bar specimen. The extrapolated value (0.3866 for $a_0/R_0=0$) of Eq. (13) (see in Fig. 15 (a)) is very close to the slope (0.3718) by linearly fitting the ratio between the true stress-strain curve from smooth round bar specimen and the input stress-strain curve for perfectly plastic material; while the extrapolated value (1.0577 for $a_0/R_0=0$) of Eq. (14) is very close to 1, giving reasonable indication that there is no stress concentration for smooth round bar specimen. However, since the proposed correction function applies to the whole range of the $\sigma_{T,notch}-\varepsilon$

curve. For the smooth round bar specimen before diffuse necking, the true stress-strain curve is exactly the same as material's equivalent stress-strain curve and no correction is needed. Application of Eq. (15) to smooth round bar specimen may results in considerable error, especially when the strain is large.

5. Verification and discussion

To verify the proposed correction function, the axisymmetric notched tensile specimen with $a_0/R_0 = 1.25$ has been analyzed numerically. The equivalent stress-strain curves calculated by converting the true stress-strain curves from the axisymmetric notched tensile specimen with Eq. (16) are compared in Fig. 16 with the materials' equivalent stress-strain curves. Very satisfactory agreement can be seen in Fig. 16 for materials with $n = 0$ and $n = 0.125$. Compared with the well-known Bridgman correction method, the proposed correction function does not need to measure the current notch radius. Gromada et al. (2011) performed the Bridgman correction method with the perfectly plastic material numerically, and found that errors between the Bridgman corrected stress and the material's equivalent stress occurred quite early and increased to 10% at the strain $\varepsilon = 1.25$. Compared with the Bridgman correction method, the proposed correction function yields accurate results for the perfectly plastic material, as can be seen in Fig. 16 (a).

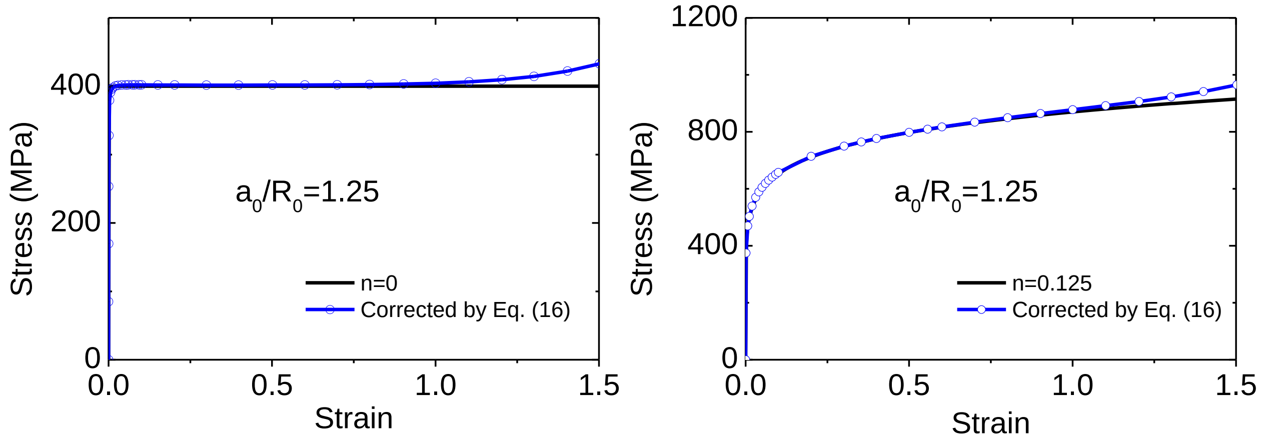

(a) (b)

Fig. 16 Comparison of the equivalent stress-strain curve calculated by correcting the trues stress-strain curve from the axisymmetric notched tensile specimen with the proposed correction function and the material's equivalent stress-strain curve: (a) $n = 0$ *; (b)* $n = 0.125$ *.*

It should be noted that the conversion of the true stress-train curve from the axisymmetric notched tensile specimens to the material's equivalent stress-strain curve with the proposed correction function is not perfect when the strain is very small. Fig.16 is replotted by ranging strain from 0 to 0.01 in Fig. 17. Difference between the equivalent stress-strain curves converted by the proposed correction function and the material's equivalent stress-strain curves is shown in Fig. 17. One reason for the errors is that the normalized $\xi - \varepsilon$ curves in Fig. 7 (b)-12 (b) are linearly fitted, however, the normalized ξ deviates slightly to the linearly fitted equation in the initial stage. The second reason is that the transition of yielding for the notched tensile specimen is different to the smooth specimen. Yielding develops on the whole cross-section simultaneously for the smooth specimen, while the yielding for the axisymmetric notched tensile specimen develops firstly at part of the minimum cross-section. Gradual yielding of the axisymmetric notched tensile specimens also results in a smooth transition on the converted equivalent stress-strain curve, instead of a sharp transition in a smooth round bar specimen.

In practice, for tensile tests with smooth round bar specimen or rectangular cross-section specimen, the yield stress is determined by the intersection of the 0.2% offset line ($\sigma_{0.2}$) or the vertical line at the strain 0.5% ($\sigma_{0.5}$) on the equivalent stress-strain curve, for materials without obvious yield plateau (ASTM E8/E8M-16a). In this study, both $\sigma_{0.2}$ and $\sigma_{0.5}$ are derived from both the corrected equivalent stress-strain curve and the material's equivalent stress-strain curve for all the analyses in section 4, see in Fig. 17 as an example. The relative errors (absolute value) are presented in Table 2 for $\sigma_{0.2}$ and Table 3 for $\sigma_{0.5}$, respectively.

It can be seen that the values of the relative errors in table 2 and table 3 are within 5%, except the data marked in red which are mainly from the axisymmetric notched tensile specimen with $a_0/R_0 = 2$ and $a_0/R_0 = 3$. Therefore, it is not recommended to use very sharp axisymmetric notched tensile specimen to measure material's yield stress on the converted equivalent stress-strain curve with the proposed correction function.

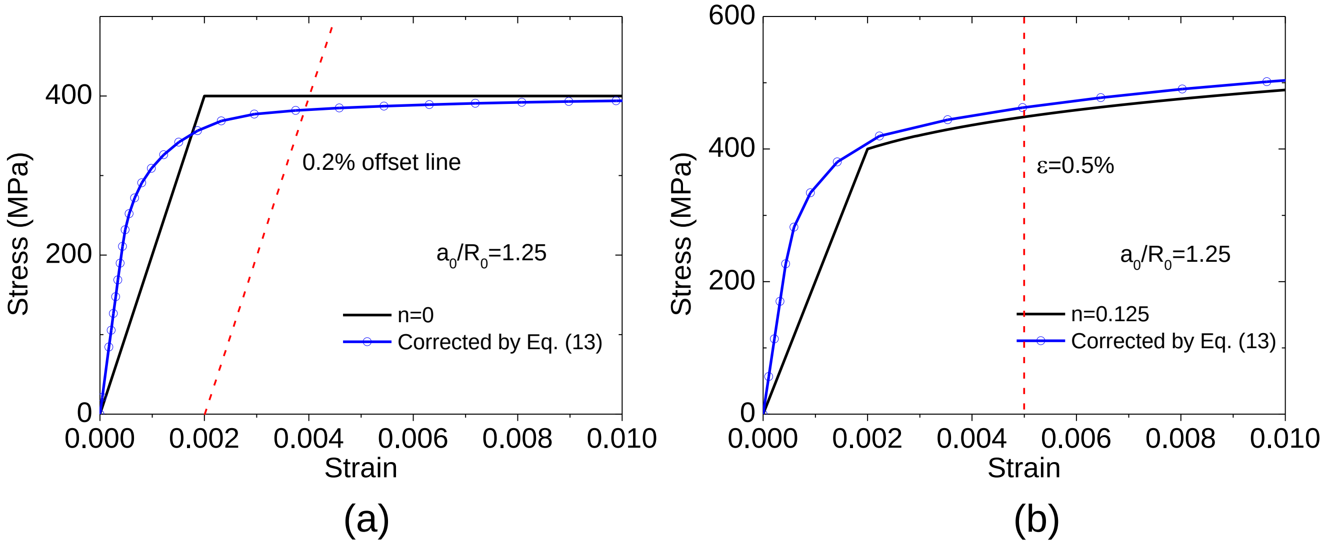

Fig. 17 Converted equivalent stress-strain curve by the proposed correction function at the strain less than 1% for materials with : (a) $n=0$ *; (b)* $n=0.125$.

Table 2 Absolute value of Relative error of the 0.2% offset yield stress ($\sigma_{0.2}$*)*

n	a_0/R_0					
	0.25	**0.5**	**1**	**1.5**	**2**	**3**
0	0.018	0.013	0.025	0.05	0.08	0.121
0.05	0.005	0.008	0.018	0.046	0.049	0.083
0.1	0.008	0.011	0.008	0.032	0.064	0.101
0.15	0.03	0.031	0.011	0.016	0.044	0.078
0.2	0.046	0.045	0.027	0.023	0.021	0.049

Table 3 Absolute value of Relative error of the yield stress at $\varepsilon=0.5\%$ *(*$\sigma_{0.5}$*)*

n	a_0/R_0					
	0.25	**0.5**	**1**	**1.5**	**2**	**3**
0	0.013	0.006	0.015	0.035	0.059	0.098
0.05	0.007	0.003	0.016	0.039	0.025	0.051
0.1	0.002	0.005	0.013	0.033	0.055	0.086
0.15	0.019	0.017	0	0.021	0.042	0.069
0.2	0.032	0.032	0.018	0.003	0.022	0.043

Since not all the materials follow power law hardening rule, the true stress-strain curves from smooth round bar specimen for steel 20MnMoNi 55 [16], AISI 304 and FE 430 [17] have been used to verify the correction function. The true stress-strain curves are expressed as Eq. (17)-(19) and are converted to equivalent stress-strain curves with the so-called MLR method introduced in [16]. The correction factor for the MLR method can be expressed as Eq. (20):

For steel 20MnMoNi 55:

$$\sigma_T = \begin{cases} 828 \cdot \varepsilon^{0.1} & \text{for } (0 < \varepsilon \le 0.1) \\ 614 + 460 \cdot \varepsilon & \text{for } (\varepsilon > 0.1) \end{cases} \tag{17}$$

For steel AISI 304:

$$\sigma_T = \begin{cases} 1183 \cdot \varepsilon^{0.25} & \text{for } (0 < \varepsilon \le 0.25) \\ 693 + 592 \cdot \varepsilon & \text{for } (\varepsilon > 0.25) \end{cases} \tag{18}$$

For steel FE 430:

$$\sigma_T = \begin{cases} 818 \cdot \varepsilon^{0.19} & \text{for } (0 < \varepsilon \le 0.19) \\ 527 + 365 \cdot \varepsilon & \text{for } (\varepsilon > 0.19) \end{cases} \tag{19}$$

$$MLR\sigma\left(\varepsilon, \varepsilon_N\right) = 1 - 0.6058(\varepsilon - \varepsilon_N)^2 + 0.6317(\varepsilon - \varepsilon_N)^3 - 0.2107(\varepsilon - \varepsilon_N)^4 \tag{20}$$

where ε_N is the true strain at diffuse necking, which can be found in ref. [16] and [17]. By multiplying the true stress with the MLR correction factor, the equivalent stress-strain curve can be derived after diffuse necking. It should be noted that the error induced by the MLR is not considered here. The equivalent stress-strain curves converted by the MLR method are then converted to flow stress-strain curves and are input for numerical analyses with different axisymmetric notched tensile specimens. True stress-strain curves from the numerical analyses are then corrected with the proposed correction function, Eq. (15), up to the same failure strain as in ref. [16] and [17]. Results of the corresponding equivalent stress-strain curves converted by the proposed correction function from numerical analyses as well as the MLR converted equivalent stress-strain curves are presented in Fig. 18. For the application of Eq. (15), the true strain at the maximum tensile load is obtained from the force-true strain curve for each material and each specimen geometry and is presented in Table 4.

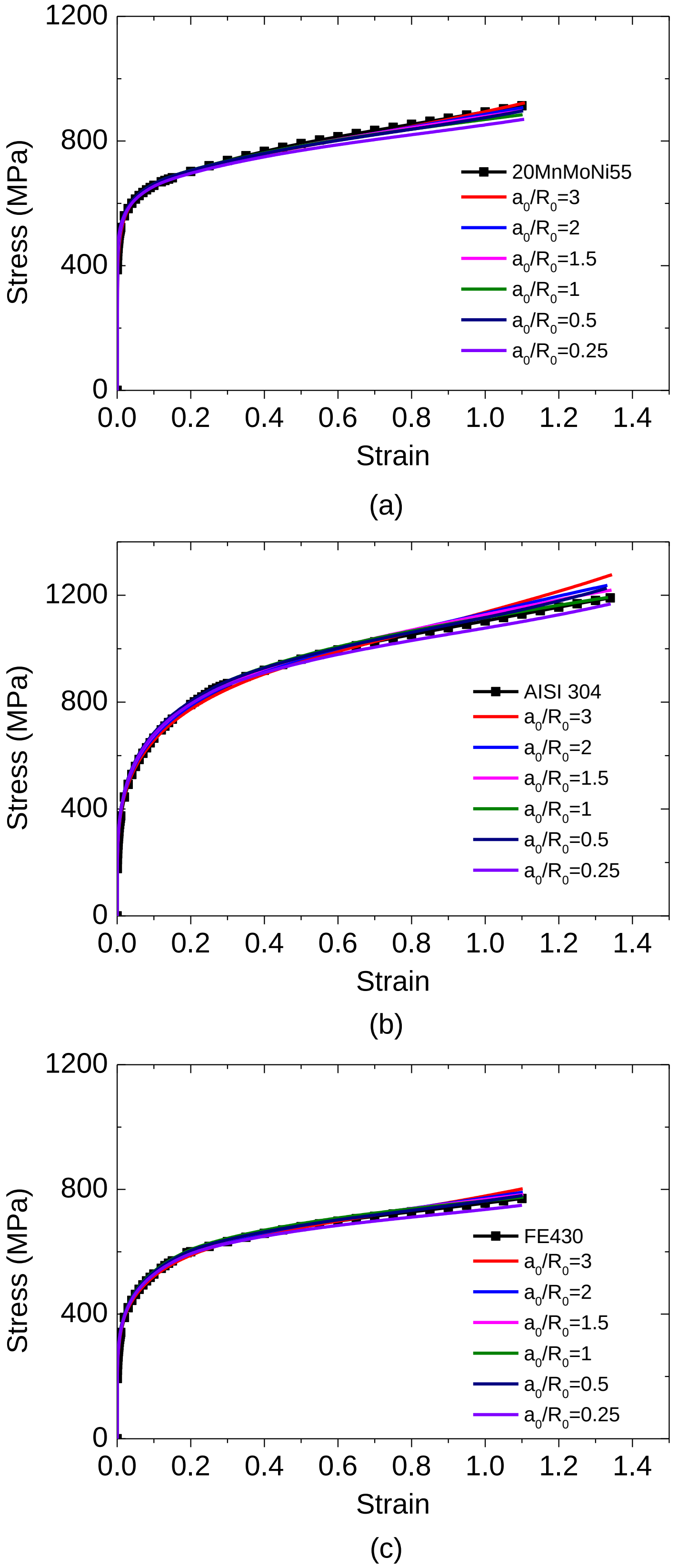

Fig. 18 Comparison of the equivalent stress-strain curves calculated by correcting the trues stress-strain curves from the axisymmetric notched tensile specimens with the proposed correction function and the MLR corrected equivalent stress-strain curve: (a) 20MnMoNi 55; (b) AISI 304; (c) FE 430 .

Table 4 Error analysis for the application of the proposed correction function

Material	failure strain	a_0/R_0	$\varepsilon_{P\max}$	Error
20MnMoNi55	1.1	3	0.091	1.02 %
		2	0.095	0.98 %
		1.5	0.097	1.81 %
		1	0.102	3.11 %
		0.5	0.115	1.58 %
		0.25	0.12	4.75 %
AISI 304	1.33	3	0.212	7.16 %
		2	0.225	3.98 %
		1.5	0.236	2.34 %
		1	0.253	1.36 %
		0.5	0.273	3.17 %
		0.25	0.275	2.32 %
FE 430	1.1	3	0.16	4.04 %
		2	0.169	2.59 %
		1.5	0.176	1.57 %
		1	0.188	1.31 %
		0.5	0.199	0.04 %
		0.25	0.2	2.6 %

As can be seen in Fig. 18, the equivalent stress-strain curves derived from the axisymmetric notched tensile specimens with the proposed correction function agree well with the MLR corrected equivalent stress-strain curves, except small deviations. It can also be noted that difference occurs when the strain is large in Fig. 18. Errors between the equivalent stress-strain curves from notched specimens and from the MLR corrected equivalent stress-strain curves are listed in Table 4. It can be seen that most of the errors are within 5%, except the one for steel AISI 304 with $a_0/R_0 = 3$. It can also be observed that the strain at the maximum tensile load deviates slightly from the strain at necking from smooth round bar specimen.

Fig. 19 presents the results of the equivalent stress-strain curves by correcting the true stress-strain curves from notched specimens with Eq. (15), together with the reference equivalent stress-strain curve for material D98 in ref. [19]. The true stress-strain curves are calculated numerically. The reference equivalent stress-strain curve in ref. [19] was derived by correcting true stress-strain curve from smooth round bar specimen with Bridgman correction method and expressed as:

$$\sigma_{eq} = \begin{cases} 1260 \cdot \varepsilon^{0.35} & \text{for } (0 < \varepsilon \le 0.55) \\ 933 + 197 \cdot \varepsilon & \text{for } (\varepsilon > 0.65) \end{cases} \tag{21}$$

Tensile test with smooth round bar specimen in ref. [19] shows that diffuse necking occur at strain $\varepsilon = 0.35$ for this D98 material. The authors in [19] performed numerical analysis with smooth round bar specimen, using Eq. (21) as the input equivalent stress-strain curve. True stress-strain curve from numerical analysis was then corrected with Bridgman correction. They found that the equivalent stress-strain curve corrected by the Bridgman correction from numerical analysis differed with the input equivalent stress-strain curve at large strain. The error reaches up to 10.6% at the strain $\varepsilon = 1.35$. As can be seen in Fig. 19, the equivalent stress-strain curves corrected by Eq. (16) are higher than the reference curve when the strain is larger than 0.7. The errors at the strain $\varepsilon = 1.35$ range from 3.68% to 13.52%. It can also be noticed that notched specimen with larger a_0/R_0 shows larger deviation with the reference curve.

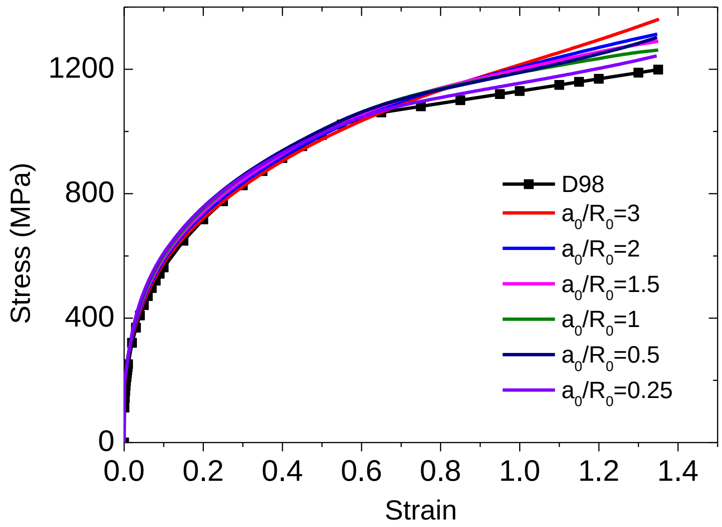

Fig. 19 Comparison of the equivalent stress-strain curves calculated from the axisymmetric notched tensile specimens with the proposed correction function and the equivalent stress-strain curve from Ref. [19].

It should be noted that notched specimen fails at smaller strain than smooth round bar specimen. The sharper (larger a_0/R_0) the notch is, the smaller the failure strain will be. This is due to the reason that the failure strain depends significantly on the stress triaxiality, which is the ratio of mean stress and Mises equivalent stress. Sharper notch corresponds to a higher stress triaxiality, resulting in a smaller failure strain. In order to obtain equivalent stress-strain curve in larger strain and considering the error analysis, we recommend to use notched specimen with smaller a_0/R_0 for the application of the proposed correction function.

The proposed correction function can also be applied to determine the equivalent stress-strain curve of each individual material zone in a weldment. By locating the notch either in the base material, weld metal, or possibly in the heat affected zone, the material's equivalent stress-strain curve in the notched region as shown in Fig. 1 can be determined with the proposed correction function, once the geometry conditions ($d_0 \geq 3.5a_0$; $a_0 \leq H$) are fulfilled.

By summarizing the results above, a recommended procedure is proposed to determine material's equivalent stress-strain curve with an axisymmetric notched tensile specimen:

1. Prepare the axisymmetric notched tensile specimen under the geometry requirements: $d_0 \geq 3.5a_0$, $a_0 \leq H$;
2. Perform tensile test with the axisymmetric notched tensile specimen, record the load and the minimum cross section diameter;
3. Calculate the $\sigma_{T,notch} - \varepsilon$ curve and the $\sigma_{e,notch} - \varepsilon$ curve, determine $\varepsilon_{P\max}$ on the $\sigma_{e,notch} - \varepsilon$ curve;
4. With the data of the initial notch radius ratio a_0/R_0 and $\varepsilon_{P\max}$, convert the $\sigma_{T,notch} - \varepsilon$ curve by Eq. (16) to derive the material's equivalent stress-strain curve.

6. Conclusions

Recently, we identified a so-called 'magic' special axisymmetric notched tensile specimen to derive material's flow stress-strain curve for hardening material [21]. In this study, we proposed a correction function by performing a series of numerical analyses with axisymmetric notched tensile specimens. With the proposed correction function, the true stress-strain curve from any axisymmetric notched tensile specimen can be converted to the material's equivalent stress-strain curve and no Bridgman correction is needed. Accordingly, a recommended procedure to determine the material's equivalent stress-strain curve with the axisymmetric notched tensile specimens is proposed. The proposed procedure can be used to hardening materials, as well as perfectly plastic material. Furthermore, the proposed procedure can be applied to both homogeneous material and inhomogeneous materials (such as the weldment), by locating the notch in the target material zone under the geometry requirements ($d_0 \geq 3.5a_0$, $a_0 \leq H$). The proposed procedure is cheap and accurate, since the only information needed to record during the tensile test is load and minimum cross section area (radius).

Acknowledgement

The Chinese Scholarship Council is greatly acknowledged for the financial support. The authors wish to thank the Research Council of Norway for funding through the Petromaks 2 Programme, Contract No.228513/E30.

Reference

[1] F.M. Andrade Pires, J.M.A. César de Sá, L. Costa Sousa, R.M. Natal Jorge, Numerical modelling of ductile plastic damage in bulk metal forming, International Journal of Mechanical Sciences, 45 (2003) 273-294.

[2] O.M. Badr, F. Barlat, B. Rolfe, M.-G. Lee, P. Hodgson, M. Weiss, Constitutive modelling of high strength titanium alloy Ti-6Al-4 V for sheet forming applications at room temperature, International Journal of Solids and Structures, 80 (2016) 334-347.

[3] Z. L, Zhang, C. Thaulow, J. Ødegård, A complete Gurson model approach for ductile fracture, Engineering Fracture Mechanics, 67 (2000) 155-168.

[4] Z.L. Zhang, A sensitivity analysis of material parameters for for the Gurson constitutive model, Fatigue & Fracture of Engineering Materials & Structures, 19 (1996) 561-570.

[5] J. Xu, Z.L. Zhang, E. Østby, B. Nyhus, D.B. Sun, Constraint effect on the ductile crack growth resistance of circumferentially cracked pipes, Engineering Fracture Mechanics, 77 (2010) 671-684.

[6] J. Xu, Z.L. Zhang, E. Østby, B. Nyhus, D.B. Sun, Effects of crack depth and specimen size on ductile crack growth of SENT and SENB specimens for fracture mechanics evaluation of pipeline steels, International Journal of Pressure Vessels and Piping, 86 (2009) 787-797.

[7] A. Dunbar, X. Wang, W.R. Tyson, S. Xu, Simulation of ductile crack propagation and determination of CTOAs in pipeline steels using cohesive zone modelling, Fatigue & Fracture of Engineering Materials & Structures, 37 (2014) 592-602.

[8] Z.L. Zhang, M. Hauge, J. Ødegård, C. Thaulow, Determining material true stress-strain curve from tensile specimens with rectangular cross-section, International Journal of Solids and Structures, 36 (1999) 3497-3516.

[9] I. Scheider, W. Brocks, A. Cornec, Procedure for the determination of true stress-strain curves from tensile tests with rectangular cross-section specimens, Journal of Engineering Material and Technology, 126 (2004) 70-76.

[10] M. Joun, J.G. Eom, M.C. Lee, A new method for acquiring true stress–strain curves over a large range of strains using a tensile test and finite element method, Mechanics of Materials, 40 (2008) 586-593.

[11] Z.L. Zhang, J. Ødegård, O.P. Søvik, Determining true stress-strain curve for isotropic and anisotropic materials with rectangular tensile bars: method and verifications, Computational Materials Science, 20 (2001) 77-85.

[12] W.J. Yuan, Z.L. Zhang, Y.J. Su, L.J. Qiao, W.Y. Chu, Influence of specimen thickness with rectangular cross-section on the tensile properties of structural steels, Materials Science and Engineering: A, 532 (2012) 601-605.

[13] Z.L. Zhang, M. Hauge, C. Thaulow, J. Ødegård, A notched cross weld tensile testing method for determining true stress–strain curves for weldments, Engineering Fracture Mechanics, 69 (2002) 353-366.

[14] J. Choung, Comparative studies of fracture models for marine structural steels, Ocean Engineering, 36 (2009) 1164-1174.

[15] M. Gromada, G. Mishuris, Andreas, Correction formulae for the stress distribution in round tensile specimens at neck presence, Springer, 2011.

[16] G. Mirone, A new model for the elastoplastic characterization and the stress–strain determination on the necking section of a tensile specimen, International Journal of Solids and Structures, 41 (2004) 3545-3564.

[17] G. Mirone, D. Corallo, A local viewpoint for evaluating the influence of stress triaxiality and Lode angle on ductile failure and hardening, International Journal of Plasticity, 26 (2010) 348-371.

[18] P.W. Bridgman, Studies in large plastic flow and fracture, MaGraw-Hill, New York, 1952.

[19] G. La Rosa, G. Mirone, Risitano. A, Postnecking elastoplastic characterization degree of approximation in the bridgman method and properties of the flow stress true stress ratio, Metallurgical and Materials Transactions A, 34 (2003) 615-624.

[20] Y. Bao, Dependence of ductile crack formation in tensile tests on stress triaxiality, stress and strain ratios, Engineering Fracture Mechanics, 72 (2005) 505-522.

[21] S. Tu, X. Ren, B. Nyhus, O.M. Akselsen, J. He, Z. L. Zhang, A special notched tensile specimen to determine the flow stress-strain curve of hardening materials without applying the Bridgman correction, Engineering Fracture Mechanics, 179 (2017) 225-239.

[22] T. Børvik, O.S. Hopperstad, T. Berstad, On the influence of stress triaxiality and strain rate on the behaviour of a structural steel. Part II. Numerical study, European Journal of Mechanics - A/Solids, 22 (2003) 15-32.

[23] T. Børvik, O.S. Hopperstad, S. Dey, E.V. Pizzinato, M. Langseth, C. Albertini, Strength and ductility of Weldox 460 E steel at high strain rates, elevated temperatures and various stress triaxialities, Engineering Fracture Mechanics, 72 (2005) 1071-1087.

[24] O.S. Hopperstad, T. Børvik, M. Langseth, K. Labibes, C. Albertini, On the influence of stress triaxiality and strain rate on the behaviour of a structural steel. Part I. Experiments, European Journal of Mechanics - A/Solids, 22 (2003) 1-13.

[25] H. Yu, J.S. Olsen, A. Alvaro, V. Olden, J. He, Z. L. Zhang, A uniform hydrogen degradation law for high strength steels, Engineering Fracture Mechanics, 157 (2016) 56-71.

[26] Y. Bao, T. Wierzbicki, On fracture locus in the equivalent strain and stress triaxiality space, International Journal of Mechanical Sciences, 46 (2004) 81-98.

[27] Y. Bao, T. Wierzbicki, On the cut-off value of negative triaxiality for fracture, Engineering Fracture Mechanics, 72 (2005) 1049-1069.

[28] H. Yu, J.S. Olsen, J. He, Z. L. Zhang, Effects of loading path on the fracture loci in a 3D space, Engineering Fracture Mechanics, 151 (2016) 22-36.

[29] Z.L. Zhang, M. Hauge, C. Thaulow, Two parameter characterization of the near-tip stress field for a bi-material elastic-plastic interface crack, International Journal of Fracture, 79 (1996) 65-83.

[30] ASTM E8/E8M-16a Standard test method for tension test of metallic materials, in, ASTM International, West Conshohocken, PA, 2016.